

4.4. PHYTOPLANKTON AND PRIMARY PRODUCTIVITY OFF NORTHWEST AFRICA

Hervé DEMARCQ¹ and Laila SOMOUE²

¹ Institut de Recherche pour le Développement. France

² Institut National de Recherche Halieutique. Morocco

4.4.1. INTRODUCTION

Eastern boundary upwelling ecosystems (EBUEs) cover less than 2% of the ocean surface, but contribute 7% of the global marine production. Upwelling systems are a major source of the net primary production (NPP) in tropical and subtropical latitudes and sustain the most productive pelagic fisheries of the world, accounting for 20% to 30% of global marine fisheries production (FAO, 2012a).

The Canary Current Upwelling System (CCUS), which extends from the Iberian Peninsula to Guinea (43°N to 8°N), is one of the most productive coastal upwelling system in the world. It covers the whole Canary Current Large Marine Ecosystem (CCLME). This EBUE is maintained by intense equatorward trade winds (see Soares, 3.1 this volume), persistent in the central part of the region and seasonal in the southern and northern parts, in winter and summer respectively. The wind stress drives offshore surface transport compensated by an inshore and progressively upward flux of nutrient-rich water masses. This upwelling process is adequately modeled by the Ekman transport (Bakun, 1973; Ekman, 1905), used earlier to describe the average seasonal cycle of upwelling in the region (Schemainda et al., 1975; Wooster et al., 1976).

The nutrient concentrations reaching the euphotic layer directly govern the intensity of the phytoplankton blooms during the year (see for example Huntsman and Barber, 1977), simultaneously controlled by the sun light at the sea surface and its vertical penetration.

Phytoplankton are composed of a large diversity of unicellular algae or bacterias and form the base of the marine food web, that constraints all life in the oceans, up to its super-predator part, mostly driven by human consumption through commercial fisheries (Chassot et al., 2010; Watson et al., 2014).

Primary production is the synthesis of organic matter from atmospheric or dissolved carbon dioxide (CO₂), a process that occurs through photosynthesis, a way of harvesting light to convert inorganic carbon to organic carbon. Phytoplankton are mostly composed of photoautotrophic organisms, called primary producers, which are passively transported in water masses. They ultimately supply organic carbon to diverse heterotrophic organisms that obtain their energy solely from the oxydation of organic matter.

Primary production can be considered as net (NPP) or gross (GPP), depending if carbon losses from the respiration of the autotrophic organisms are included. Integrated within the euphotic zone, where sunlight penetrates, the “net ecosystem production” (NEP) from all living organisms is equivalent to the sinking organic carbon, in both particulate or dissolved form.

Despite contributing only 1-2% of the global primary biomass on earth (Falkowski, 1994; Field et al., 1998), oceanic productivity ($\pm 40 \text{ GtC yr}^{-1}$) accounts for about 40% of the total NPP.

This article reviews the various factors that drive NPP in upwelling systems in general and in the CCUS in particular, as well as some ways to estimate it. Quantitative estimates are presented from a remote sensing-based model and the spatio-temporal patterns of productivity are described. The plankton diversity of the region, as detailed from *in situ* determinations in the Moroccan region is also described.

4.4.2. OCEANIC PRIMARY PRODUCTIVITY AND THE GLOBAL CARBON CYCLE

CO₂ concentrations have increased by 40% since pre-industrial times (year 1750) (IPCC, 2013) and more than 25% from any time in the past 420,000 years (Petit et al., 1999). One of the major changes in the global carbon cycle on earth is that the role of the oceans has become predominant. The oceans are now a net sink of CO₂, by removing 2.3 ± 0.7 PgC yr⁻¹ from the atmosphere (i.e. about 26% of the anthropogenic emissions), a value similar (2.6 ± 1.2 PgC yr⁻¹) to that of the terrestrial biosphere (IPCC, 2013). It is also estimated that this sink has increased only slightly over the last two decades (Sitch et al., 2015; Wanninkhof et al., 2013), probably because the global temperature increase has reduced the efficiency of the ocean to dissolve CO₂.

Ultimately, only 25% of the carbon fixed in the upper ocean sinks into the interior where it is oxidized by heterotrophic organisms (Falkowski et al., 1998; Laws et al., 2000). This is achieved by the sinking of organic matter before it is returned to dissolved inorganic carbon and dissolved nutrients by bacterial decomposition. Oceanographers often refer to this process as the "biological pump", as it pumps CO₂ out of the surface of the ocean and atmosphere into the voluminous deep ocean (Volk and Hoffert, 1985).

The ocean response to climate change, and particularly the response of EBUEs, that account for 7% of the global marine production, is of primary importance in quantifying the carbon cycle and the way human impacts continue to modify it.

4.4.3. FACTORS LIMITING PRODUCTIVITY

Phytoplankton growth and productivity are affected by several "limiting" factors, including nutrients, light, temperature, circulation, grazing and other biological constraints (Eppley, 1972; Tilman et al., 1982) within the euphotic zone, the upper part of the epipelagic province (0-200m) where light penetrates.

4.4.3.1. Upwelling intensity and nutrient availability

Because of the importance of physical forcing in upwelling systems, the first factor of variability is the supply of nutrient-rich waters to the surface, in direct relationship with the local intensity of the upwelling (see Pelegrí and Benazzouz, 3.4 this volume). The variable width of the continental shelf of the CCUS and the presence of several Capes (from north to south, Cape Ghir, Cape Juby, Cape Bojador and Cape Blanc, see Figure 4.4.1.), contribute to the variable upwelling intensity between different regions, according to the local orientation of the coast line. The resulting enrichment is proportional to the essential nutrient concentrations of the upwelled water that will be used by the phytoplankton in the form of nitrate, phosphate and silicates (see Pelegrí and Peña-Izquierdo, 4.1 this volume).

As described by Tomczak and Hughes (1980) and Barton (1998) the surface waters of the CCUS are formed from North Atlantic Central Water (NACW, 11.00-18.65°C, 35.47-36.76‰ defined by Sverdrup et al. (1942) that dominates the upwelled waters North of Cape Blanc (20°N) in association with deeper intermediate

Eastern North Atlantic Central Water (ENACW, 8.0-18.0°C, 35.2-36.7 ‰ defined by Fiuza and Halpern, 1982). South Atlantic Central Water (SACW, 35.70‰ and 9.70°C, 35.177‰ and 15.25°C), with 3 times higher average nutrient concentration (Fraga, 1974) dominates the southern part of the system, strongly enhancing enrichment of the upwelling system south of Cape Blanc. Coastal upwelling has been shown to be dominated by nitrate-based production, whereas ammonium-based production becomes progressively dominant further offshore: on the shelf off Cape Blanc, Barber and Smith (1981) estimated that regenerated nitrogen accounted for 72% of total nitrogen, whereas close to Cape Ghir, Head et al. (1996) showed bacterial consumption to account for 50% of the total NPP.

4.4.3.2. Light limitation

The second important factor controlling primary production is the availability of sunlight, characterized by daily and seasonal changes in intensity and duration. Sunlight penetrates the semi-transparent water of the euphotic zone, generally defined as the depth where light reaches 1% of its surface value and where photosynthesis occurs. The depth of the euphotic layer varies from less than 10 m in dense or turbid coastal waters to about 80 m in very oligotrophic waters, as those of the tropical oceanic gyres.

An important limit is the “compensation depth” (Sverdrup, 1953), where the rate of photosynthesis exactly matches the rate of respiration, and beyond which no NPP can occur. Because of the dominance of light in phytoplankton growth in upwelling systems, this limit is generally close to the bottom of the euphotic zone.

In the Canary region, light availability is high, especially in the central – cloud free desert region with quasi permanent trade winds from 20°N to 26°N. Light availability decreases on either side of this region: in the north because of a more temperate climate with a summer light maximum, and in the south, from central Mauritania to Guinea, where light is limited in summer because of the high cloud cover due to the northernmost position of the Inter-Tropical Convergence Zone. Nonetheless, on average, the strong seasonality of light moderately impacts the photosynthesis process in the regional areas of upwelling, because of its natural co-occurrence with the trade winds. Because of this compensation effect, Head et al. (1996), did not find any correlation between integrated primary production rates and light intensity in Moroccan inshore waters, despite a two-fold variation of light between winter and summer.

In the euphotic zone, especially in rich coastal upwelling systems, light is significantly limited by self-shading, an important constraint in oceanic NPP (Steemann Nielsen et al., 1962). Mathematical models of self-shading show that settlement characteristics of each species determine, along with nutrient concentrations, the vertical distribution of phytoplankton species (Shigesada and Okubo, 1981). Various experiments support the fact that large phytoplankton species, such as diatoms, induce less self-shading than smaller phytoplankton because of their smaller chloroplast densities and therefore support higher biomasses (Agusti, 1991). Mesocosm experiments show that the self-shading by phytoplankton increasingly constrains abundance as nutrient concentrations increase (Oviatt et al., 1989), leading to a severe drop in the production:biomass (P:B) ratio. Light limitation due to self-shading therefore provides an important negative feedback to phytoplankton abundance and biomass estimation through the water column, with important implications in primary production models, that are almost always based on estimations of biomass, via chlorophyll-a.

4.4.3.3. Secondary limiting elements

The third source of enrichment is represented by elements from sources other than that of the upwelled water, but rather from either the atmosphere or from the sediments. The enrichment from atmospheric

Nitrogen (N) is very low in Northwest Africa (<0.1%) as in the case for most upwelling systems (Mackey et al., 2010) and its benefit are mostly limited to species able to fix dinitrogen gas, such as the cyanobacterium *Trichodesmium*.

At the contrary, iron, a major limiting nutrient, is supplied in the form of atmospheric aerosols. Iron is known to significantly affect phytoplankton growth and therefore oceanic productivity, especially in upwelling regions where high-N and high-P deep water is brought rapidly to the surface (Martin et al., 1988).

The CCUS, especially between Cape Bojador and Cape Blanc, is not affected by iron limitation, first because of its relatively wide continental shelf and because dust deposits coming from the Sahara Desert are very frequent (Jickells et al., 2005; Mills et al., 2004; Gelado-Caballero, 2.3 this book). Manganese, known to limit phytoplankton growth (Dawes, 1998), is also relatively abundant in the coastal waters of Northwest Africa (Shiller, 1997).

The trapping of nutrients on the shelf can be also important (Aristegui et al., 2009a) as the resuspension of sediments may contribute significantly to silicate, generally in excess North of Cape Blanc (Minas et al., 1982) but more rapidly exhausted off Mauritania (Herbland and Voituriez, 1974), where the continental shelf is relatively narrow. This positive effect is more important in the CCUS compared to other EBUEs because of its wider continental shelf, especially south of Cape Bojador (26°N). South of the Cap-Vert peninsula, the considerably nutrient-rich SACW dominates. Except in the extreme south of the system, fresh water runoff plays only a minor role in this enrichment.

4.4.3.4. Biological limitations

The competition between marine species for nutrients and light as well as the diversity of the abiotic environment primarily drives the natural diversity of phytoplankton (see i.e. Margalef, 1978). In EBUEs, this diversity is first measured by the number of species and mostly varies on a cross-shore gradient, determined by spatio-temporal succession of algae.

Zooplankton grazers can significantly decrease phytoplankton density. For example, at a grazing rate of 20%, zooplankton can decrease phytoplankton populations by approximately 75% (Dawes, 1998). On the contrary, high zooplankton grazing pressures may stimulates phytoplankton growth, due to the release of nutrient by the grazers (Strickland, 1972), whereas moderate grazing (10% daily) may produce a doubling of the growth rate (Oviatt et al., 1989). As with other factors affecting phytoplankton production, the effect of grazers is seasonal. Because grazers decline in winter, there is a lag in spring before grazers become effective in controlling spring blooms. For these reasons, the way grazing pressure is integrated into production biogeochemical models is of high importance in their tuning (Hashioka et al., 2013) and in determining the dominance of major phytoplankton groups.

4.4.4. METHODS FOR ESTIMATING PRIMARY PRODUCTION

Whereas the term “primary production” represents a cumulative amount of biomass produced during a given period of time, the term referring to the measurement of a biomass increase over time is “primary productivity”. It is defined as “the rate at which solar energy is converted into chemical energy by photosynthetic and chemosynthetic organisms” (Dillon and Rodgers, 1980), and it is usually expressed as grams of carbon fixed per unit area per unit of time (Dawes, 1998).

The under-sampling of ship-based estimates of global NPP requires significant extrapolation, making it essentially impossible to quantify basin-scale variability from *in situ* measurements. Fortunately, satellite observations contribute to resolving this problem, by providing synoptic measures of ocean color (McClain, 1998). Numerous satellite-based production models exist, either at regional or global scales. A review of the comparison of most models can be found in Carr et al. (2006).

Biogeochemical models, coupled to numerical ocean circulation models (not described here), are also extremely useful in understanding processes in oceans, complementing direct observations. Experiments with the Regional Ocean Modeling System - Pelagic Interaction Scheme for Carbon and Ecosystem Studies (ROMS-PISCES) coupled model are presently set up for the CCUS, but to date only aspects of physical modeling (Marchesiello and Estrade, 2007) have been published. Lagrangian experiments to study the passive drift of planktonic eggs and larvae have been undertaken by Brochier et al. (2008).

Models generally include one or two phytoplankton (and zooplankton) compartments, in order to discriminate between diatom-like large cell species (micro-phytoplankton) and small cells species (nano-plankton). The Dynamic Green Ocean Model (DGOM) is a biogeochemical model that integrates 6 distinct phytoplankton groups (Le Quéré et al., 2005), while some recent models (Goebel et al., 2010) between 50 and 100, based on a reduced number of functional groups. An overview on the scope and history of ocean biogeochemical models can be found in Doney et al. (2003).

4.4.4.1. Direct measurements

The first quantitative studies of primary productivity in the Canary EBUE, made with direct measurements of C14 uptake (first introduced by Steeman-Nielsen, 1952), were mostly made during the 70s (Barber and Smith, 1981; Coste and Minas, 1982; Huntsman and Barber, 1977; Minas et al., 1986; Minas et al., 1982) in March and April 1974 (CINECA-*Charcot V* cruise), in the Cape Blanc region between 21°N and 22°N, the most consistently productive part of the CCLME. Huntsman and Barber (1977) measured NPP values consistently between 1 gC m⁻² d⁻¹ and 3 gC m⁻² d⁻¹, except in inshore areas where it was assumed that turbidity limited light penetration. Minas et al. (1982) measured values between 0.7 gC m⁻² d⁻¹ and 4.7 gC m⁻² d⁻¹ during the same cruise from a different set of stations in the same area. This large variability is reinforced by the fact that Cape Blanc is located within the mixing region between NACW and SACW. The strong differences in nutrient concentration, combined with the high mesoscale activity of this area (see Sangrà, 3.5. this book) probably explain the large difference in productivity within a relatively small area.

The yearly integrated coastal NPP in the Cape Blanc region has been estimated at 750 gC m⁻² yr⁻¹ (Longhurst et al., 1995), a value similar to those estimated from remote sensing-based production models.

4.4.4.2. Remote sensing-based production models

The era of ocean color observation from space started with the experimental Coastal Zone Color Scanner (CZCS) on board of the Nimbus-7 spacecraft launched in 1978 by the National Aeronautics and Space Administration (NASA). By accurately measuring ocean pigment concentrations (mostly chlorophyll-a), this sensor supplied precious data to the international scientific community until 1986. This was followed by the long-awaited Sea-viewing Wide Field-of-view Sensor (SeaWiFS) in 1997 (data up to 2010 but continuously up to December 2007) and by the MODerate resolution Imaging Spectroradiometer (MODIS) instrument in June 2002, that still operates. More recently (January 2012) the Visible Infrared Imaging Radiometer Suite (VIIRS) instrument has extended and improved the measurements initiated by the MODIS sensor.

Data from platforms other than those operated by NASA have also been successfully used and include the MEdium Resolution Imaging Spectrometer (MERIS) sensor from the European Space Agency (ESA), on board the Envisat platform, between 2002 and 2012.

Standard algorithm-derived ocean color products encompass turbidity, dissolved organic carbon, particulate inorganic carbon, natural fluorescence, etc., but the most widely used product is by far chlorophyll-a (Figure 4.4.1). Because of its specific absorption in the blue and red parts of the visible light, chlorophyll-a algorithms are derived from ratios of light reflected from the sea surface in the blue and green parts of the visible spectra. Chlorophyll-a is the major natural pigment used by plants and unicellular algae to produce chemical energy from sun light through photosynthesis. Therefore, its quantitative estimation from space allows the construction of production models of different complexity, provided that the knowledge of intermediate variables such as the sunlight reaching the sea surface (specifically photosynthetically active radiation – PAR - also estimated from satellite measurements of cloud coverage), the water temperature and various physiological parameters can be estimated, at least for the main groups of algae present in the oceans. Of course, mineral nutrients and temperature (that strongly affects metabolic rates) play crucial roles in regulating NPP in the ocean.

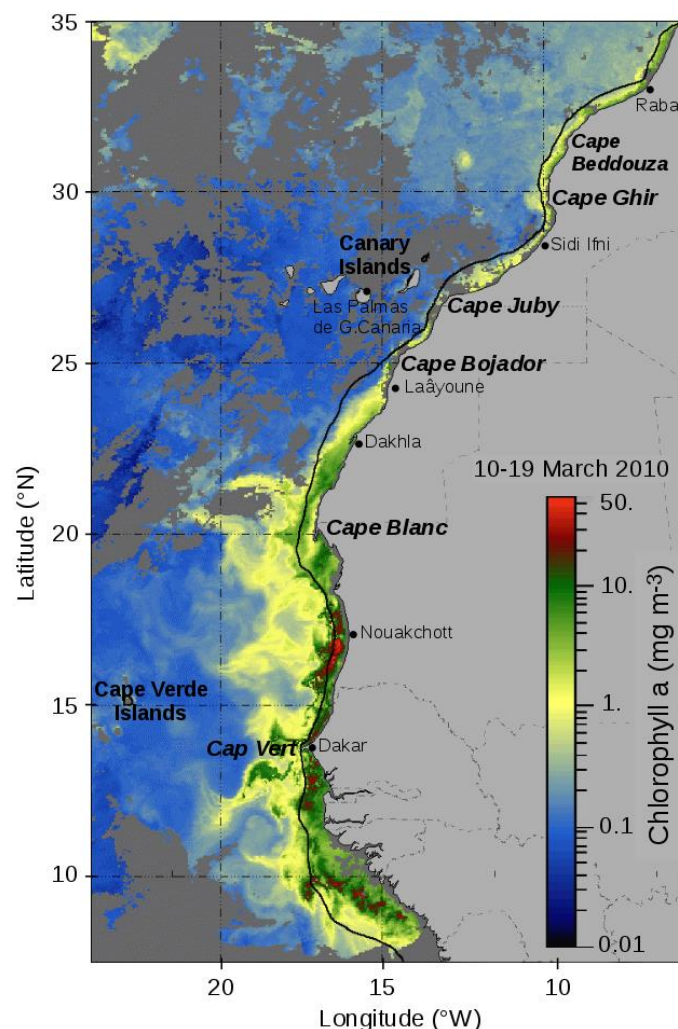


Figure 4.4.1. Average chlorophyll-a computed from MODIS sensor data for the period 10-19 March 2010, during the maximum southward extension of the trade winds concomitant of the maximum intensity of the Mauritanian-Senegalese upwelling. The 200 m bathymetry contour (black line) is added.

For these reasons, remote sensing data provide a powerful source of information by measuring ocean optical properties from which phytoplankton biomass and productivity can be derived (Feldman et al., 1989; Longhurst et al., 1995). Photosynthesis models of varying complexity have been used worldwide (Behrenfeld and Falkowski, 1997; Morel and Berthon, 1989; Platt and Sathyendranath, 1993).

These models integrate numerous uncertainties related to the estimations of the physiological parameters of the models, such as the carbon:chlorophyll ratio of the different groups of algae, the growth rate of cells according to light and temperature, parameters that vary strongly according to the main functional groups of phytoplankton. Nevertheless, thanks to the availability of continuous fields of chlorophyll-a measured from space, production models provide an unprecedented synoptic view of the oceanic productivity. Size-fractionated production models (Kameda and Ishizaka, 2005; Uitz et al., 2012) integrate various empirical relationships between remote sensing variables in order to split the primary production into its different size classes (micro, nano, and picophytoplankton). Remote sensing of phytoplankton functional types from ocean color (Aiken et al., 2009; Alvain et al., 2008; Hirata et al., 2008; Mustapha et al., 2014; Nair et al., 2008) is also an emerging field, that helps to better understand (for the moment mostly at global scale) the importance of the environment in structuring the marine phytoplankton diversity as well as the mechanisms favouring four different functional types of algae: Synechococcus-like-cyanobacteria, diatoms, Prochlorococcus, Nanoeucaryotes (such as dinoflagellates) and Phaeocystis-like.

In 4.4.5, we show some results from SeaWiFS data, from chlorophyll-a estimates and a generic production model.

4.4.5. PRODUCTIVITY PATTERNS IN THE CCUS

A simple calculation based on SeaWiFS data of chlorophyll-a concentration (a proxy for the phytoplankton biomass) from 1998 to 2007 shows that despite representing only 1.5% of the oceanic surface between 45°S and 45°N, upwelling systems account for 9.3% of the biomass of primary producers.

This computation is based on the limit of 0.5 mg of chlorophyll-a as the best limit to delineate the productive part of the upwelling region as used in previous studies (Demarcq et al., 2007; Nixon and Thomas, 2001). Based on the same chlorophyll-a data, the primary biomass of all four major upwelling systems is approximately 6 times higher than the average of the biomass outside upwelling regions, in the same latitude range of 45°S to 45°N.

Within the same four main upwelling systems, comparative studies (Carr, 2001) show that the CCUS, with a value of 0.33 GtC yr⁻¹ would be the second most productive system after the Benguela Current (0.37 GtC yr⁻¹), followed by the Humboldt (0.20 GtC yr⁻¹) and California systems (0.04 GtC yr⁻¹).

The spatio-temporal seasonality of the NPP is computed from the Vertically Generalized Production Model (VGPM) of Behrenfeld and Falkowski (1997). As for most models using chlorophyll-based biomasses, this model estimates NPP from surface chlorophyll using a temperature-dependent description of chlorophyll-specific photosynthetic efficiency and also assumes that phytoplankton biomass is related to a single formulation equating depth-integrated NPP to satellite-measured surface biomass. The other variables are the photoadaptive variable of the maximum production rate under saturating light, the depth of the euphotic zone, the irradiance-dependent function and day length.

The seasonality of the NPP is represented by the monthly averages from all SeaWiFS data from 1998 to 2007 (Figure 4.4.2). It shows high seasonality with minimum productivity in December and a maximum in April-May. Compared to the chlorophyll-a signal from the biomass (see Figure 4.4.1), the production is forced by light (minimum in December and maximum in June) that significantly increases the seasonal contrast. The Figure 4.4.3 shows the average yearly production: (a) as well as the latitudinal/time evolution of the productive areas, first in a qualitative way; (b) by averaging the production values from the coast up to the variable offshore position of the value $1 \text{ gC m}^{-2} \text{ d}^{-1}$ (first contour line on Figure 4.4.3a); and second by a more integrated biomass index (c) from the coast to a fixed offshore distance of 500 km, e.g. approximately the distance of a latitude/longitude square on Figure 4.4.3a.

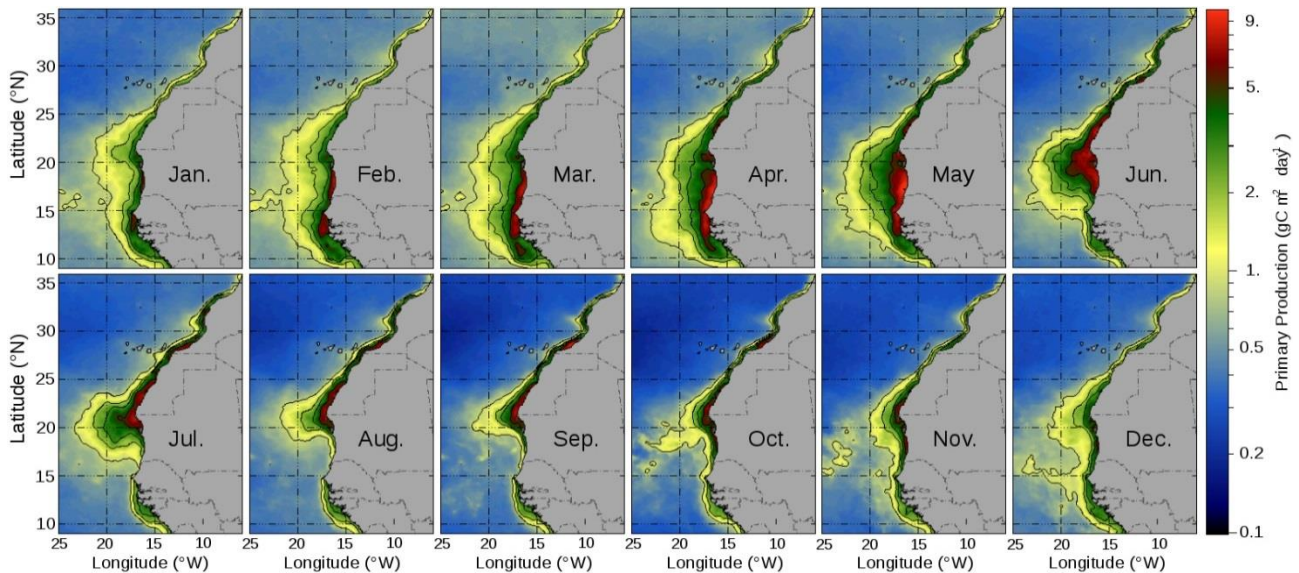


Figure 4.4.2. Seasonal variability of the NPP in the Canary Current from Morocco to Guinea, computed from SeaWiFS data, from 1998 to 2007 (VGPM algorithm, Behrenfeld and Falkowsky, 1998). Values $1 \text{ gC m}^{-2} \text{ d}^{-1}$, $2 \text{ gC m}^{-2} \text{ d}^{-1}$, $3 \text{ gC m}^{-2} \text{ d}^{-1}$ and $5 \text{ gC m}^{-2} \text{ d}^{-1}$ are contoured.

The progressive displacement of the most productive areas (values greater than $5 \text{ gC m}^{-2} \text{ d}^{-1}$) is clearly visible, with a local coastal maximum in Senegal and southern Mauritania from January to May, a maximum in north Mauritania in June that progressively decreases up to December, whereas southern Senegal and Guinea (10°N - 15°N) maintain stable average levels (around $2 \text{ gC m}^{-2} \text{ d}^{-1}$) over the shelf without any upwelling, probably because of the importance of the nutrients from the wide and shallow continental shelf, in addition to nutrient input from several rivers.

Because of the narrowness of the continental shelf, in the central part of the system (from 20°N to 26°N) high levels of productivity show a moderate offshore extension. On the contrary, the region off Cape Blanc (20°N - 21°N) shows a strong offshore extension of a constantly windy productive zone, characterized by a giant filament described by several authors (Fischer et al., 2009; Gabric et al., 1993; Meunier et al., 2012).

As mentioned above, the southern part of the system (9°N - 21°N) is clearly the most productive (despite a less intense wind regime than the central part, from 21°N to 26°N) because of the exceptional nutrient content of SACW (Fraga, 1974), with enrichment extending as far as the Cape Verde archipelago.

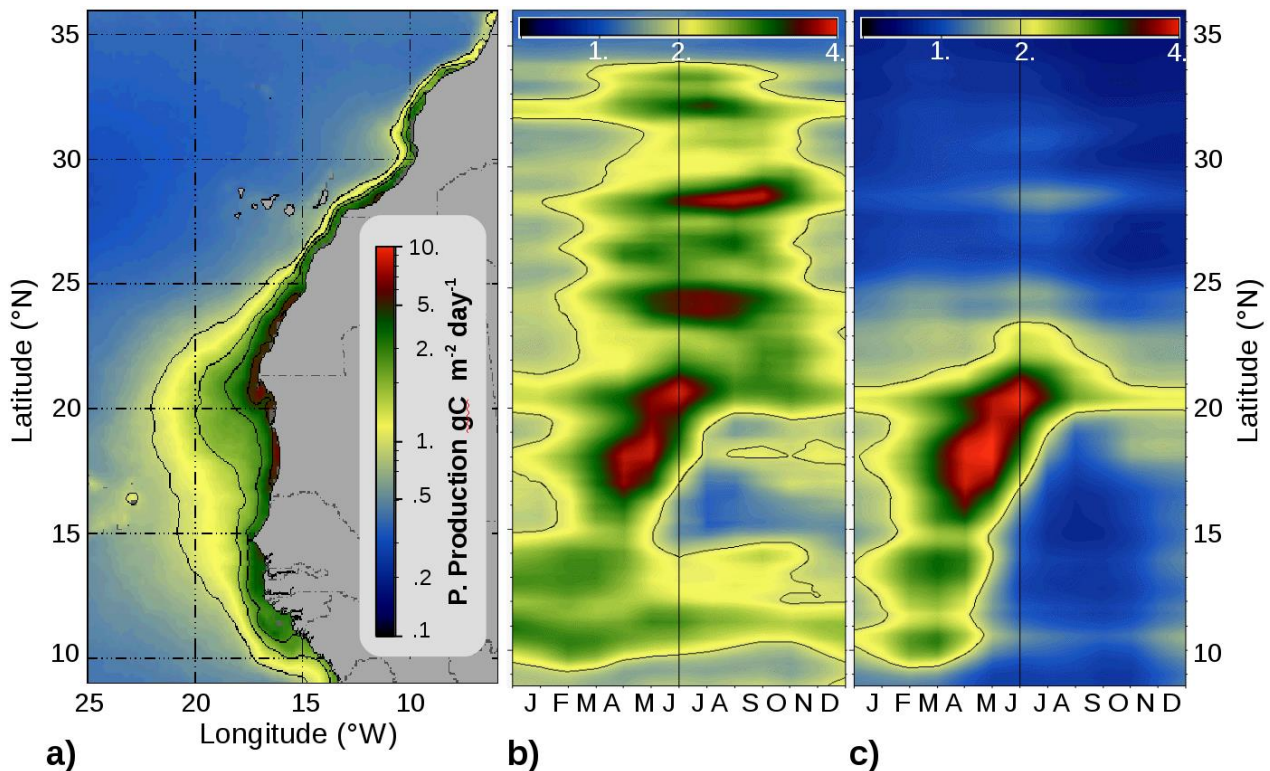


Figure 4.4.3. a) Annual average of the NPP (VGMP model), values $1 \text{ gC m}^{-2} \text{ d}^{-1}$, $2 \text{ gC m}^{-2} \text{ d}^{-1}$ and $3 \text{ gC m}^{-2} \text{ d}^{-1}$ are contoured, b) local average from the coast to the value $1 \text{ gC m}^{-2} \text{ d}^{-1}$ (most distant contour in Figure 4.4.2a), c) integrated Zonal average from the coast to 500 km. All values are in $\text{gC m}^{-2} \text{ d}^{-1}$. Isovalue $2 \text{ gC m}^{-2} \text{ d}^{-1}$ is contoured in b) and c).

4.4.6. PHYTOPLANKTON DIVERSITY AND DOMINANT SPECIES

It is recognized that marine phytoplankton diversity worldwide is relatively high, with approximately 4000 species and 500 genera described (Sournia et al., 1991) and probably much more to discover, especially in the bacterial pico-plankton ($0.2\text{-}2 \mu\text{m}$) division. This diversity is higher in freshwater systems, with 15,000 species (Bourrelly, 1985), because of the greater range of environmental conditions.

It has been suggested that this diversity is mostly controlled by the diversity of water masses (Tett and Barton, 1995) and that species richness in phytoplankton is not related to the total productivity of ecosystems (Cermeño et al., 2013). This is particularly true in coastal upwelling systems, where the diversity decreases with the distance from shore.

In upwelling systems, where diatoms dominate because of their competitive advantages in exploiting turbulent waters, they are responsible for $\approx 40\%$ of the NPP and up to 50% of the organic carbon exported to the ocean interior (Dugdale and Wilkerson, 1998).

High-Performance Liquid Chromatography (HPLC) pigment analysis in the northern Moroccan system (Head et al., 1996) showed that when chlorophyll biomass was high, diatoms were dominant, whereas when it was low, small prymnesiophytes (mostly coccolithophorids), chlorophytes and diatoms were all important. Following upwelling events, the rich diatom-dominated coastal waters are progressively replaced by small flagellates (Arístegui et al., 2004; García-Muñoz et al., 2004), as nitrate is consumed and the system becomes more stratified and progressively replaced by a microbial-dominated system.

Goebel et al. (2013) used a biogeochemical model in the California Current (Goebel et al., 2010) that incorporates a high biodiversity of 78 phytoplanktonic groups. Historical observations (Capone et al., 2008; Head et al., 1996; Wilkerson et al., 2000) confirm the dominance of diatoms in nearshore upwelling regions, but more importantly these biogeochemical models are able to reproduce selectivity processes that explain the local dominance of a relatively low diversity of fast growing diatom species, whereas intermediate offshore and oligotrophic surface waters are characterized by a lower productivity and a much higher diversity (Goebel et al., 2013).

Determinations of phytoplankton species are undertaken on a yearly basis by Institut National de Recherche Halieutique (INRH, Morocco) (Somoue, 2004). Cell counts are performed with the Utermöhl method (Utermöhl, 1958) by settling 10 ml samples and concentration are expressed in cells l^{-1} . Relative abundances by species and groups are expressed from the relative percentage of individuals.

The microphytoplankton is composed of diatoms, dinoflagellates, silicoflagellates, euglenophytes, coccolithophorids and raphidophytes. It has been found that diatoms regularly dominate the central part of the Coastal upwelling from Cape Blanc to Cape Beddouza ($21^{\circ}N$ to $32^{\circ}30'N$) with relative abundances of 70-80%, followed by dinoflagellates (10-20%). The other groups are less dominant, both qualitatively and quantitatively (Elghrib et al., 2012; Somoue, 2004; Somoue et al., 2003).

Numerous authors (Margalef, 1978; Smayda and Trainer, 2010; Tilstone et al., 2000), have shown the diatom:dinoflagellate ratio to be closely dependent of the vertical mixing of the water column. Dinoflagellates need for example relatively well stratified waters for optimal growth whereas diatoms have a high ability to be maintained in turbulent water masses (Tilstone et al., 2000), thanks to their extremely high rates of nitrate uptake, leading to maximal growth rates of 1 day^{-1} , even with low iron concentrations (Sunda et al., 1991).

For these reasons upwelling systems are tightly structured by their underlying physical processes: flux of upwelled water, turbulence, offshore displacement and stratification of aged upwelling waters, light penetration, etc. These factors are summarized in Figure 4.4.4.

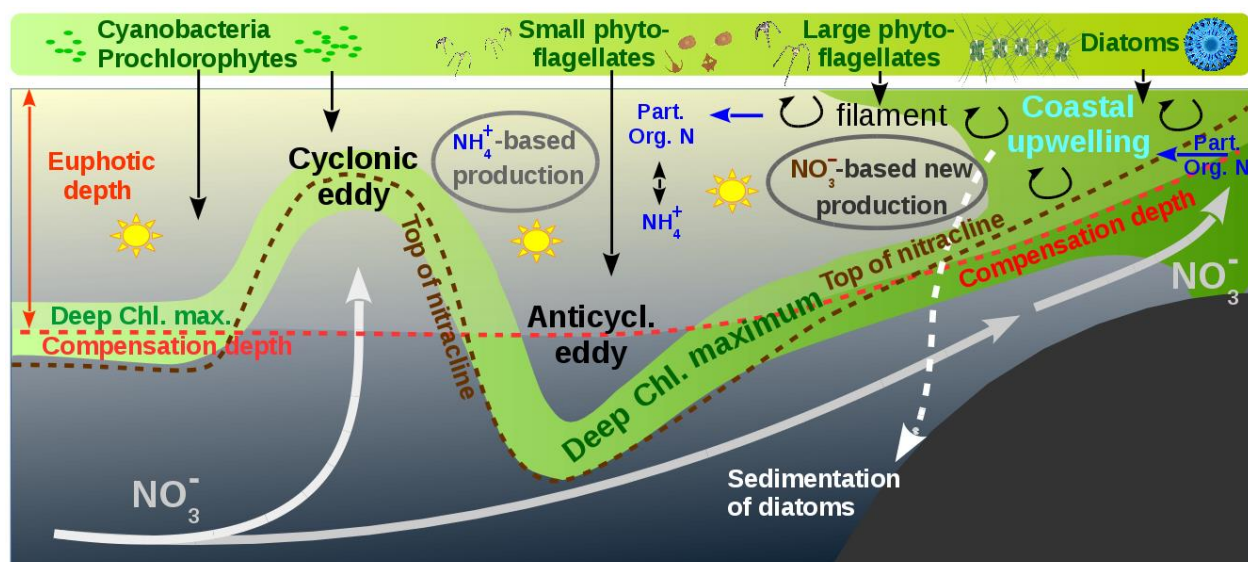


Figure 4.4.4. Schematic representation of the cross-shore section of an upwelling system, from coastal NO_3^- based new production to NH_4^+ based regenerated production, with the influence of the main limiting factors (nutrients and light). The upper rectangle represents the typical size-decreasing algae succession (based in Barton et al., 1998).

In Moroccan waters, 217 taxa of micro-phytoplankton have been identified (Elghrib et al., 2012; Somoue, 2004) from Cape Blanc (21°N) to Cape Beddouza (32°30'N). All taxa are listed in Table 4.4.1. The most abundant diatoms are *Chaetoceros* spp., *Leptocylindrus danicus*, *Leptocylindrus minimus*, *Pseudonitzschia* spp., *Thalassiosira* spp., *Melosira* spp. and *Nitzschia* spp. The most common dinoflagellates are: *Protoperidinium* spp., *Alexandrium* spp., *Prorocentrum* spp. and *Gymnodinium* spp. Their relative abundance varies according to the depth and distance from upwelling centers, and according to season and region, mostly because of differences in the local intensity of coastal upwelling (Makaoui et al., 2005).

In the Senegalese upwelling system, historical and partial measurements in December 1981 and March 1982 (Dia, 1986) have shown 5 dominant species present in most locations during the upwelling season (*Thalassionema nitzschioides*, *Pleurosigma elongatum*, *Hemiaulus sinensis*, *Chaetoceros decipiens* and *Rhizosolenia hyalina*) and 5 other species mostly during the onset of the upwelling season, in December (*Nitzschia seriata*, *Chaetoceros affine*, *Chaetoceros curvisetum*, *Rhizosolenia stolterfothii* and *Skeletonema costatum*). Only the two later species are still present at the end of the upwelling season. Due to the coastal position of most stations, dinoflagellates have been more rarely observed. Nevertheless, 5 dinoflagellates species have been recorded during the upwelling season. In Senegal, among 38 diatom species and 6 dinoflagellate species, diatoms represent 93% of the biomass of all species.

4.4.7. CONCLUSIONS AND RECOMMENDATIONS

The knowledge of carbon cycling in the CCUS is dominated by process studies conducted off the Iberian Peninsula, while the knowledge of the diversity of phytoplankton is mostly the consequence of studies from the Iberian and the Moroccan regions.

Extremely few studies concern the southern, yet most productive part of the system, either from a qualitative or quantitative point of view.

At all scales explored, the way productivity is distributed in space and time is directly related to the physics of the upwelling. For example, a nutrient maximum is generally observed 2 to 4 days after a coastal upwelling event and the induced production generally 3 to 10 days after the event and may be sustained for 2-3 days (Jones and Halpern, 1981).

Remote sensing-based observations and modeling are presently the only way to report in both time and space the short-term dynamics of coastal upwelling and its mesoscale structures, as well as to integrate the whole production of the system in space or time.

Combined with process studies, still very scarce in the southern part of the system, a continuous modeling effort would greatly help to better understand the various processes involved in the productivity of the CCUS as well as in the whole CCLME, in order to manage fishing activities in the long term and to preserve still relatively poorly known – albeit heavily exploited – regions of the system.

Table 4.4.1. List of microphytoplankton taxa recorded from Cape Blanc to Cape Beddouza (21°N- 32°30'N).

Diatoms	
<i>Achnanthes brevipes</i> Agardh, 1824	<i>Hemiaulus</i> spp.
<i>Achnanthes</i> spp.	<i>Hemidiscus</i> spp.
<i>Amphora</i> spp.	<i>Hyalodiscus radiatus</i> (O'Meara) Grunow, 1880
<i>Asterionellopsis glacialis</i> (Castracane) Round, 1990	<i>Lauderia annulata</i> Cleve, 1873
<i>Asterolampra</i> spp.	<i>Leptocylindrus danicus</i> Cleve, 1889
<i>Bacteriastrum</i> spp.	<i>Leptocylindrus mediterraneus</i> (Peragallo) Hasle, 1975
<i>Bellerocha</i> spp.	<i>Leptocylindrus minimus</i> Gran, 1915
<i>Cerataulina</i> spp.	<i>Licmophora ehrenbergii</i> (Kützing) Grunow, 1867
<i>Chaetoceros convolutus</i> Castracane, 1886	<i>Licmophora</i> spp.
<i>Chaetoceros danicus</i> Cleve, 1889	<i>Lyrella</i> spp.
<i>Chaetoceros decipiens</i> Cleve, 1873	<i>Melosira</i> spp.
<i>Chaetoceros densus</i> (Cleve) Cleve, 1899	<i>Navicula neoventricosa</i> Hustedt, 1966
<i>Chaetoceros didymus</i> Ehrenberg, 1845	<i>Navicula</i> spp.
<i>Chaetoceros eibenii</i> (Grunow) Van Heurck, 1880-1885	<i>Nitzschia longissima</i> (Brébisson) Ralfs, 1861
<i>Chaetoceros peruvianus</i> Brightwell, 1856	<i>Nitzschia rectilonga</i> Takano, 1983
<i>Chaetoceros socialis</i> Lauder, 1864	<i>Nitzschia</i> spp.
<i>Chaetoceros</i> spp.	<i>Odontella</i> spp.
<i>Climacodinium frauenfeldianum</i> Grunow, 1868	<i>Opephora</i> spp.
<i>Corethron pennatum</i> (Grunow) Ostefeld, 1909	<i>Paralia sulcata</i> (Ehrenberg) Cleve, 1873
<i>Coscinodiscus curvulatus</i> Schmidt, 1878	<i>Plagiodiscus martensianus</i> Grunow & Eulenstein
<i>Coscinodiscus</i> spp.	<i>Plagiotropis</i> spp.
<i>Ceratoneis closterium</i> Ehrenberg, 1839	<i>Planktoniella</i> spp.
<i>Dactyliosolen fragilissimus</i> (Bergon) Hasle, 1996	<i>Pleurosigma directum</i> Grunow, 1880
<i>Detonula</i> spp.	<i>Pleurosigma normanii</i> Ralfs, 1861
<i>Diploneis bombus</i> (Ehrenberg) Ehrenberg, 1853	<i>Pleurosigma</i> spp.
<i>Diploneis crabro</i> (Ehrenberg) Ehrenberg, 1854	<i>Podosira stelligera</i> (Bailey) Mann, 1907
<i>Diploneis</i> spp.	<i>Proboscia alata</i> (Brightwell) Sundström, 1986
<i>Ditylum brightwellii</i> (West) Grunow, 1885	<i>Psammodictyon panduriforme</i> (Gregory) Mann, 1990
<i>Entomoneis</i> spp.	<i>Pseudo-nitzschia heimii</i> Manguin, 1957
<i>Epithemia</i> spp.	<i>Pseudo-nitzschia pungens</i> (Grunow ex Cleve) Hasle, 1993
<i>Eucampia cornuta</i> (Cleve) Grunow, 1883	<i>Pseudo-nitzschia seriata</i> (Cleve) Peragallo, 1899
<i>Eucampia</i> spp.	<i>Pseudo-nitzschia delicatissima</i> (Cleve) Heiden, 1928
<i>Eucampia zodiacus</i> Ehrenberg, 1839	<i>Pseudo-nitzschia</i> spp.
<i>Fragilaria</i> spp.	<i>Rhizosolenia acicularis</i> Sundström, 1986
<i>Gomphonema</i> spp.	<i>Rhizosolenia antennata</i> (Ehrenberg) Brown, 1920
<i>Gossleriella tropica</i> Schütt	<i>Rhizosolenia bergonii</i> Peragallo, 1892
<i>Grammatophora marina</i> (Lyngbye) Kützing, 1844	<i>Rhizosolenia clevei</i> var. <i>communis</i> Sundström, 1984
<i>Guinardia cylindrus</i> (Cleve) Hasle, 1996	<i>Rhizosolenia curvata</i> Zacharias, 1905
<i>Guinardia delicatula</i> (Cleve) Hasle, 1997	<i>Rhizosolenia hebetata</i> f. <i>semispina</i> (Hensen) Gran, 1905
<i>Guinardia flaccida</i> (Castracane) Peragallo, 1892	<i>Rhizosolenia imbricata</i> Brightwell, 1858
<i>Guinardia</i> sp.	<i>Rhizosolenia polydactyla</i> Castracane, 1886
<i>Guinardia striata</i> (Stolterfoth) Hasle, 1996	<i>Neocalyptrella robusta</i> (Norman ex Ralfs) Hernández-Becerril & Meave del Castillo, 1997
<i>Gyrosigma</i> spp.	<i>Rhizosolenia setigera</i> Brightwell, 1858
<i>Hantzschia amphioxys</i> (Ehrenberg) Grunow, 1880	<i>Rhizosolenia setigera</i> f. <i>pungens</i> (Cleve-Euler) Brunel, 1962
<i>Helicotheca tamesis</i> (Shrubsole) Ricard, 1890	<i>Rhizosolenia simplex</i> Karsten, 1905
<i>Hemiaulus proteus</i> Heiberg, 1863	<i>Rhizosolenia styliformis</i> Brightwell, 1858
<i>Hemiaulus hauckii</i> Grunow ex Van Heurck, 1882	<i>Roperia</i> spp.
<i>Hemiaulus sinensis</i> Greville, 1865	<i>Skeletonema costatum</i> (Greville) Cleve, 1873

Diatoms	
<i>Skeletonema</i> spp.	<i>Thalassionema nitzschoides</i> (Grunow) Mereschkowsky, 1902
<i>Stephanopyxis palmeriana</i> (Greville) Grunow, 1884	<i>Thalassionema pseudonitzschooides</i> (Schuette & Schrader) Hasle
<i>Suirella</i> spp.	<i>Thalassionema</i> spp.
<i>Striatella</i> spp.	<i>Thalassiosira</i> spp.
<i>Striatella unipunctata</i> (Lyngbye) Agardh, 1832	<i>Thalassiothrix longissima</i> Cleve & Grunow, 1880
<i>Terpsinoë musica</i> Ehrenberg, 1843	<i>Tryblionella compressa</i> (Bailey) Poulin, 1990
<i>Thalassionema javanicum</i> (Grunow) Hasle	<i>Trigonium</i> spp.

Dinoflagellates	
<i>Amphidinium</i> spp.	<i>Neoceratium declinatum</i> (Karsten) Gomez, Moreira & Lopez-Garcia, 2010
<i>Alexandrium</i> spp.	<i>Neoceratium furca</i> (Ehrenberg) Gomez, Moreira & Lopez-Garcia, 2010
<i>Archaeoperidinium minutum</i> (Kofoid) Jörgensen, 1912	<i>Neoceratium fusus</i> (Ehrenberg) Gomez, Moreira & Lopez-Garcia, 2010
<i>Cochlodinium</i> spp.	<i>Neoceratium horridum</i> (Gran) Gomez, Moreira & Lopez-Garcia, 2010
<i>Ceratium</i> spp.	<i>Neoceratium lineatum</i> (Ehrenberg) Gomez, Moreira & Lopez-Garcia, 2010
<i>Coolia monotis</i> Meunier, 1919	<i>Neoceratium macroceros</i> (Ehrenberg) Gomez, Moreira & Lopez-Garcia, 2010
<i>Dinophysis acuminata</i> Claparède & Lachman, 1859	<i>Neoceratium pentagonum</i> (Gourret) Gomez, Moreira & Lopez-Garcia, 2010
<i>Dinophysis acuta</i> Ehrenberg, 1839	<i>Neoceratium symmetricum</i> (Pavillard) Gomez, Moreira & Lopez-Garcia, 2010
<i>Dinophysis caudata</i> Saville-Kent, 1881	<i>Neoceratium trichoceros</i> (Ehrenberg) Gomez, Moreira & Lopez-Garcia, 2010
<i>Dinophysis fortii</i> Pavillard, 1923	<i>Neoceratium tripos</i> (Müller) Gomez, Moreira & Lopez-Garcia, 2010
<i>Dinophysis infundibulis</i> Schiller, 1928	<i>Noctiluca scintillans</i> (Macartney) Kofoid & Swezy, 1921
<i>Dinophysis odiosa</i> (Pavillard) Tai & Skogsberg, 1934	<i>Peridinium quinquecorne</i> Abé, 1927
<i>Dinophysis rudgei</i> Murray & Whitting, 1899	<i>Peridiniella</i> spp.
<i>Dinophysis</i> spp.	<i>Phalacroma oxytoxoides</i> (Kofoid) Gomez, Lopez-Garcia & Moreira, 2011
<i>Diplopsalis</i> spp.	<i>Phalacroma</i> spp.
<i>Dissodinium pseudocalani</i> (Gonnert) Drebes ex Elbrächter & Drebes, 1978	<i>Pentapharsodinium dalei</i> Indelicato & Loeblich III, 1986
<i>Goniodoma</i> spp.	<i>Preperidinium meunieri</i> (Pavillard) Elbrächter, 1993
<i>Gonyaulax</i> spp.	<i>Pronoctiluca</i> spp.
<i>Gymnodinium catenatum</i> Graham, 1943	<i>Prorocentrum cordatum</i> (Ostenfeld) Dodge, 1975
<i>Gymnodinium</i> spp.	<i>Prorocentrum emarginatum</i> Fukuyo, 1981
<i>Gyrodinium fissum</i> (Levander) Kofoid & Swezy, 1921	<i>Prorocentrum gracile</i> Schütt, 1895
<i>Gyrodinium spirale</i> (Bergh) Kofoid & Swezy, 1921	<i>Prorocentrum lima</i> (Ehrenberg) Stein, 1878
<i>Gyrodinium</i> spp.	<i>Prorocentrum mexicanum</i> Osorio-Tafall, 1942
<i>Heterocapsa circularisquama</i> Horiguchi, 1995	<i>Prorocentrum micans</i> Ehrenberg, 1834
<i>Heterocapsa</i> spp.	<i>Prorocentrum rostratum</i> Stein, 1883
<i>Karenia mikimotoi</i> (Miyake & Kominami ex Oda) Hansen & Moestrup, 2000	<i>Prorocentrum</i> spp.
<i>Katodinium glaucum</i> (Lebour) Loeblich III, 1965	<i>Prorocentrum triestinum</i> Schiller, 1918
<i>Katodinium</i> spp.	<i>Protoceratium</i> spp.
<i>Ostreopsis</i> spp.	<i>Protoperidinium acanthophorum</i> (Balech) Balech, 1974
<i>Oxytoxum mediterraneum</i> Schiller	<i>Protoperidinium areolatum</i> (Peters) Balech, 1974
<i>Oxytoxum</i> spp.	<i>Protoperidinium bipes</i> (Paulsen) Balech, 1974
<i>Oxytoxum tessellatum</i> (Stein, 1883) Schütt, 1895	<i>Protoperidinium compressum</i> (Abé) Balech, 1974
<i>Neoceratium candelabrum</i> (Ehrenberg) Gómez, Moreira & López-Garcia, 2010	<i>Protoperidinium conicum</i> (Gran) Balech, 1974

Dinoflagellates	
<i>Protooperidinium denticulatum</i> (Gran & Braarud) Balech, 1974	<i>Protooperidinium</i> spp.
<i>Protooperidinium depressum</i> (Bailey) Balech, 1974	<i>Protooperidinium steinii</i> (Jørgensen) Balech, 1974
<i>Protooperidinium diabolium</i> (Cleve) Balech, 1974	<i>Protooperidinium tuba</i> (Schiller) Balech, 1974
<i>Protooperidinium divergens</i> (Ehrenberg) Balech, 1974	<i>Protoceratium reticulatum</i> (Claparède & Lachmann) Butschli, 1885
<i>Protooperidinium mastophorum</i> (Balech) Balech, 1974	<i>Pyrocystis lunula</i> (Schütt) Schütt, 1896
<i>Protooperidinium ovum</i> (Schiller) Balech, 1974	<i>Pyrocystis</i> spp.
<i>Protooperidinium pellucidum</i> Bergh ex Loeblich Jr. & Loeblich III, 1881	<i>Pyrophacus</i> spp.
<i>Protooperidinium pentagonum</i> (Gran) Balech, 1974	<i>Scrippsiella</i> spp.
<i>Protooperidinium punctulatum</i> (Paulsen) Balech, 1974	<i>Torodinium robustum</i> Kofoid & Swezy, 1921
<i>Protooperidinium pyriforme</i> (Paulsen) Balech, 1974	

Coccolithophorids	Raphidophyceae
<i>Coccolithus</i> spp.	<i>Chatonella</i> spp.
<i>Discosphaera tubifer</i> (Murray & Blackman) Ostenfeld, 1900	
<i>Pleurochrysis</i> spp.	Silicoflagellates
<i>Rhabdosphaera clavigera</i> Murray & Blackman, 1898	<i>Dictyocha fibula</i> Ehrenberg, 1839
<i>Zygosphaera</i> spp.	<i>Dictyocha speculum</i> Ehrenberg, 1839
	<i>Dictyocha crux</i> Ehrenberg, 1840
Euglenophyceae	<i>Distephanus polyactis</i> var. <i>literatus</i> Bukry
<i>Euglena</i> spp.	<i>Dictyocha</i> spp.
<i>Eutreptia</i> spp.	<i>Octactis octonaria</i> (Ehrenberg) Hovasse, 1946
<i>Eutreptiella</i> spp.	

Acknowledgments

We are grateful to the NASA Ocean color team (<http://oceancolor.gsfc.nasa.gov/>, accessed on 27 April 2015) for providing the SeaWiFS data and to the Oregon State University (OSU) (<http://www.science.oregonstate.edu/ocean.productivity/>, accessed 27 April 2015) for providing the SeaWiFS derived VGPM data used in this study. We are also grateful to the team of the biological oceanography laboratory of INRH for providing the taxa observations.



United Nations
Educational, Scientific and
Cultural Organization



Intergovernmental
Oceanographic
Commission



Technical Series 115

Oceanographic and biological features in the Canary Current Large Marine Ecosystem

Intergovernmental Oceanographic Commission of UNESCO (IOC-UNESCO)



UNESCO's Intergovernmental Oceanographic Commission (IOC), established in 1960, promotes international cooperation and coordinates programmes in marine research, services, observation systems, hazard mitigation, and capacity development in order to understand and effectively manage the resources of the ocean and coastal areas. By applying this knowledge, the Commission aims to improve the governance, management, institutional

capacity, and decision-making processes of its 147 Member States with respect to marine resources and climate variability and to foster sustainable development of the marine environment, in particular in developing countries. The Commission responds, as a competent international organisation, to the requirements deriving from the United Nations Convention on the Law of the Sea (UNCLOS), the United Nations Conference on Environment and Development (UNCED), and other international instruments relevant to marine scientific research, related services and capacity-building.

Instituto Español de Oceanografía (IEO)



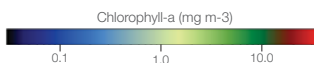
The Spanish Institute of Oceanography (IEO), founded in 1914, is a public research body attached to the Ministry of Economy and Competitiveness. The IEO is dedicated to marine science research, especially in relation to scientific knowledge of the ocean, sustainable marine living resources and fisheries, aquaculture and the marine environment. The IEO is committed to addressing the challenges facing the ocean for the benefit of society and is also an advisory institution on oceanographic research, ocean health and conservation and fish stock management for the Spanish government. The IEO networks with the Spanish scientific community, as well as partner organizations in many countries; it also fosters a long-standing commitment to international cooperation with developing countries aimed to ensure the sustainable use of marine resources and the oceanographic research. The IEO represents Spain in most intergovernmental science and technology forums related to the ocean and its resources such as the Intergovernmental Oceanographic Commission of UNESCO (IOC-UNESCO), the International Council for the Exploration of the Sea (ICES), the Mediterranean Science Commission (CIESM), and the Committee for the Eastern Central Atlantic Fisheries (CECAF) among others.

Spanish Agency for International Development Cooperation (AECID)



AECID, the Spanish Agency for International Cooperation for Development, is a public entity under the Ministry of Foreign Affairs and Cooperation, in charge of the coordination of the Spanish policy on international cooperation for development, aimed to the reduction of poverty and the achievement of sustainable human development. Since its foundation in 1988, the Agency has established international alliances and strengthened Spain's relations with other countries and multilateral institutions such as the United Nations agencies. This work has contributed to the recognition of Spain as a reliable partner in the field of international cooperation, promotion of equitable and sustainable societies and respect for human dignity. It is also an AECID primary objective to promote and encourage the presence of Spanish experts in international organizations devoted to international cooperation such as UNESCO and other agencies in the United Nations.

Cover photo: Phytoplanktonic blooms along the coast of Northwest Africa and Iberian Peninsula, as seen from the concentration of chlorophyll-a, in March 2013, deduced from the data of the MODIS sensor. Numerous mesoscale features such as fronts and filaments can be observed. Image by Hervé Demarcq, IRD



Intergovernmental Oceanographic Commission

Technical Series 115

**Oceanographic and biological features in the
Canary Current Large Marine Ecosystem**

Editors:
Luis Valdés
Itahisa Déniz-González



United Nations
Educational, Scientific and
Cultural Organization



Intergovernmental
Oceanographic
Commission



With the support of the Spanish Agency for
International Development Cooperation (AECID)



UNESCO 2015

Disclaimer

The designations employed and the presentation of the material in this publication do not imply the expression of any opinion whatsoever on the part of the Secretariats of UNESCO and IOC concerning the legal status of any country or territory, or its authorities, or concerning the delimitation of the frontiers of any country or territory.

The authors are responsible for the choice and the presentation of the facts contained in this publication and for the opinions expressed therein, which are not necessarily those of UNESCO and do not commit the Organization.

For bibliographic purposes, this document should be cited as: Valdés, L.¹ and Déniz-González, I.¹ (eds). 2015. *Oceanographic and biological features in the Canary Current Large Marine Ecosystem*. IOC-UNESCO, Paris. IOC Technical Series, No. 115: 383 pp.

¹ Intergovernmental Oceanographic Commission of UNESCO (IOC-UNESCO), Paris, France

The publication *Oceanographic and biological features in the Canary Current Large Marine Ecosystem* is also available online at:

<http://www.unesco.org/new/en/ioc/ts115>

(IOC/2015/TS/115)